Real Time Assessment of Building Envelope Systems Subject to Hurricanes Through Kriging Metamodels

Bowei Li

Department of Civil and Environmental Engineering, University of Michigan, Ann Arbor, MI 48105, U.S.A
E-mail: jacklbw@umich.edu

Zhicheng Ouyang

Department of Civil and Environmental Engineering, University of Michigan, Ann Arbor, MI 48105, U.S.A
E-mail: ouyangzc@umich.edu

Wei-Chu Chuang

Department of Civil and Environmental Engineering, University of Michigan, Ann Arbor, MI 48105, U.S.A
E-mail: wechuang@umich.edu

Seymour M.J. Spence

Department of Civil and Environmental Engineering, University of Michigan, Ann Arbor, MI 48105, U.S.A
E-mail: smjs@umich.edu

Real time damage assessment of building systems subject to hurricanes has attracted significant interest over the past few years owing to its potential to facilitate emergency response and management. The major difficulty in its application lies in the high computational demand stemming from the need to propagate uncertainty through systems that present significant complexity. In this paper, a Kriging metamodel based rapid damage assessment methodology for building envelope systems of engineered buildings is developed to address this issue. Based on the recently proposed framework, envelope damage is characterized through progressive multi-demand coupled fragility models. Within this context, damage measures are defined for each coupled damage state of the system and a full range of uncertainties in structural properties, capacities, as well as wind load stochasticity. By calibrating the metamodels for damage prediction, deterministic mappings are defined from the input space of the site specific wind speed and direction to the output space of the means and standard deviations of the damage measures of the envelope components. The calibrated metamodels can then be used to rapidly predict the expected (with variability measured through the associated standard deviation) envelope damage in terms of predicted site specific maximum wind speed and direction, where these last are estimated in real time through parametric hurricane models. To demonstrate the applicability of the approach, a case study consisting in a 45-story steel building located in Florida is presented. The accuracy and efficiency of the proposed framework, around five orders of magnitude faster than high-fidelity models, illustrate the capability of the approach to provide real time information necessary to facilitate emergency response decision making.

Keywords: Real Time Assessment, Building Envelope, Hurricane Damage, Uncertainty Propagation, Metamodeling.

1. Introduction

Hurricane induced risks and subsequent losses have shown an increasing tendency in destructiveness over time and are reported to be amongst the costliest natural hazards to impact the built environment(Bevere and Gloor, 2020; Emanuel, 2005; Abdelhady et al., 2020). Hurricane prone areas have also experienced significant growths in their populations and economies, leading to increased vulnerability of these areas (NOAA, 2013). In this respect, real time damage assessment of building systems subject to hurricanes is of significant and growing importance for providing damage forecasts that can facilitate emergency response and management (Powell et al., 1998). Various contributions have been made towards better understanding the performance and damages sustained by building envelope systems during severe windstorms (Ouyang and Spence, 2019, 2020, 2021), however, direct application of these probabilistic frameworks in real time is still not possible, due to the large computational demand associated with the assessment process. To overcome this barrier, metamodeling approaches can be introduced. The

Proceedings of the 31th European Safety and Reliability Conference.
Edited by Bruno Castanier, Marko Cepin, David Bigaud and Christophe Berenguer

ISBN: 981-973-0000-00-0 :: doi: 10.3850/981-973-0000-00-0_esrel2021-paper

goal of these approaches is to replace the original time consuming damage assessment models with computationally cheap models therefore enabling real time assessments.

Metamodeling techniques entail defining a simpler input-output relation that is capable of providing output responses with high accuracy at a much lower computational cost as compared with high-fidelity models. Among various existing metamodeling techniques, the first and the most widely used approach is the response surface method based on polynomial regression (Box and Wilson, 1951; Towashiraporn, 2004; Seo et al., 2012; Saha et al., 2016). Despite its simple form and high efficiency, this approach may suffer from difficulty in determining the appropriate polynomial order. Particularly, an excessively high order model can lead to overfitting while an overly low order model may be insufficient to capture important local features of the high-fidelity response data. While several regression techniques have been introduced to address these issues, e.g., adaptive order scheme (Kameshwar and Padgett, 2014), piece-wise fitting (Ghosh et al., 2013), and moving least square technique (Taflanidis et al., 2013), these approaches either involve extra computational effort, or are limited to low dimensional applications. As an alternative, the Kriging approach, which is the best linear unbiased predictor (Sacks et al., 1989) that interpolates the responses at the support points while predicting variances of the prediction error, can be adopted. Different from the aforementioned regression approaches, the Kriging approach is not only highly efficient once calibrated but also interpolates the support points.

In this work, a real time assessment framework based on Kriging is developed for assessing damage to building envelope systems subject to hurricanes.

2. Building Envelope Damage Assessment Framework

In this work, building envelope damages are described by a recently proposed progressive damage assessment framework (Ouyang and Spence, 2019, 2020). Within this framework, the wind hazard is characterized by the site specific maximum hourly wind speed at the building top, $\bar{v}_H$, and associated direction, α. In defining the damage models for the building envelope system, demands in the form of dynamic inter-story drift ratios and net pressures are considered together with a series of capacities that are respectively determined for each damage state (DS) through coupled fragility analysis.

The dynamic drift demands acting on each envelope component requires the resolution of the following dynamic equilibrium:

$$\boldsymbol{M}\ddot{\boldsymbol{u}}(t) + \boldsymbol{C}\dot{\boldsymbol{u}}(t) + \boldsymbol{K}\boldsymbol{u}(t) = \boldsymbol{F}(t) \qquad (1)$$

where $\boldsymbol{M}$, $\boldsymbol{C}$, and $\boldsymbol{K}$ are respectively the structural mass, damping, and stiffness matrices; $\boldsymbol{u}(t)$, $\dot{\boldsymbol{u}}(t)$, and $\ddot{\boldsymbol{u}}(t)$ are the displacement, velocity, and acceleration vectors, respectively; $\boldsymbol{F}(t)$ is the stochastic wind load vector. Eq. (1) can be effectively solved through modal integration. In addition, the structural system is assumed to be linear elastic in Eq. (1) as typical high-rise buildings are designed to remain elastic under extreme wind events in order to satisfy life safety requirements. Despite this assumption, it is worth noting that the proposed approach can be easily extended to nonlinear systems without compromising other parts of the work. To define the fragility functions, the demand and capacity are first determined for each element of the building envelope system. In particular, each component will be subject to demands in the form of local net pressure and inter-story drift ratio, $Dr(t)$, obtained from $\boldsymbol{u}(t)$. Different from typical seismic cases, where only peak inter-story drift ratios are of interest, the entire time history of $Dr(t)$ is considered as the engineering demand parameter, edp, in order to capture the progressive nature of wind induced damages. Further, a set of sequential capacities: $\boldsymbol{C}^{Dr} = \{C_1^{Dr} \leq C_2^{Dr} \leq ... \leq C_i^{Dr} \leq ... \leq C_{N_{Dr}}^{Dr}\}$ are defined for the sequential damage states: $\{\mathrm{DS}_1^{Dr}, \mathrm{DS}_2^{Dr}, ..., \mathrm{DS}_i^{Dr}, ..., \mathrm{DS}_{N_{Dr}}^{Dr}\}$. The actual damage state induced by the inter-story drift ratio demand at time t is then determined as the highest C_i^{Dr} that has ever been exceeded by Dr before t.

The net pressure demand, on the other hand, is defined as the difference between the external and internal pressure acting on each envelope component. In particular, the external pressure is calculated by averaging the dynamic wind pressure over the outer envelope surface, while the internal pressure is estimated from the solution of the internal pressure problem in which the transient air flow at each opening is modeled through the unsteady-isentropic form of the Bernoulli equation (Vickery and Bloxham, 1992; Guha et al., 2011). For typical cladding systems, glass panels are in general the most vulnerable components with respect to failure due to net pressure. Considering that glass panels normally experience static fatigue/delayed failure, the edp for the net pressure is defined as the time evolution of the equivalent pressure, $p_{\mathrm{eq}}(t)$, for each component (Beason and Morgan, 1984). Similar to the inter-story drift ratio demand, a series of sequential capacities: $\boldsymbol{C}^p = \{C_1^p \leq C_2^p \leq ... \leq C_i^p \leq ... \leq C_{N_p}^p\}$ are defined for the sequential damage states: $\{\mathrm{DS}_1^p, \mathrm{DS}_2^p, ..., \mathrm{DS}_i^p, ..., \mathrm{DS}_{N_p}^p\}$. The actual damage state due to p_{eq} at time t is once again determined as the highest C_i^p that has ever been exceeded by $p_{\mathrm{eq}}(t)$ before t.

In practice, the capacities $\boldsymbol{C}^{Dr}$ and $\boldsymbol{C}^{p}$ are taken as random values following probability distributions defined by a corresponding set of sequential fragility functions. To further account for the coupled nature of wind-induced damage, e.g., damages caused by the inter-story drift ratio demand can lead to a decrease in the net pressure capacity and vice versa, reduction factors $\rho(t)$ are considered for the capacities of each component, which are determined by the damages occurring at time t. Within this context, a damage measure can be defined for each damage state of each vulnerable envelope component based on the demand, $edp(t)$, and associated capacity, C, as follows:

$$G_C = \frac{\min_t\{\rho(t)C - edp(t)\}}{\bar{C}} \tag{2}$$

where $\bar{C}$ is the nominal value of C.

3. Kriging Metamodeling

In the application of the aforementioned framework, it is possible to quantify the statistics (e.g., mean or standard deviation) of the damage measure G_C through Monte Carlo simulation for given $\bar{v}_H$ and α. This process, however, is in general too computationally demanding to be adopted in real time damage assessment. To address this issue, Kriging metamodels are introduced to define a deterministic mapping from the input space of $(\bar{v}_H,\ \alpha)$ to the output space of the mean, m_{G_C}, and standard deviation, σ_{G_C}, of the damage measure G_C, i.e.,

$$(\bar{v}_H,\ \alpha) \mapsto (m_{G_C},\ \sigma_{G_C}) \tag{3}$$

In the following, $y(\boldsymbol{x})$ will be used to indicate the output, e.g. m_{G_C} or σ_{G_C}, while $\boldsymbol{x}$ is defined as the input vector $[\bar{v}_H,\ \alpha]^{\mathrm{T}}$.

To define the Kriging metamodel for $\boldsymbol{x} \mapsto y$, a training data set is first determined by generating high-fidelity output samples $\boldsymbol{Y} = [y(\boldsymbol{x}_1), ..., y(\boldsymbol{x}_l), ..., y(\boldsymbol{x}_{n_\mathrm{s}})]^{\mathrm{T}}$ through the procedure presented in Section 2 at n_s predefined support points (input samples) $\boldsymbol{X} = [\boldsymbol{x}_1, ..., \boldsymbol{x}_l, ..., \boldsymbol{x}_{n_\mathrm{s}}]^{\mathrm{T}}$. The Kriging predictor $\hat{y}(\boldsymbol{x})$ is subsequently constructed from a prior Gaussian random process over the domain of $\boldsymbol{x}$ based on the training data set $(\boldsymbol{X}, \boldsymbol{Y})$:

$$\hat{y}(\boldsymbol{x}) = \boldsymbol{f}(\boldsymbol{x})^{\mathrm{T}}\boldsymbol{a} + \boldsymbol{r}(\boldsymbol{x})^{\mathrm{T}}\boldsymbol{b} \tag{4}$$

where $\boldsymbol{f}(\boldsymbol{x})$ is a set of basis functions; $\boldsymbol{r}(\boldsymbol{x}) = [R(\boldsymbol{x}, \boldsymbol{x}_1, \boldsymbol{\theta}), ..., R(\boldsymbol{x}, \boldsymbol{x}_l, \boldsymbol{\theta}), ..., R(\boldsymbol{x}, \boldsymbol{x}_{n_\mathrm{s}}, \boldsymbol{\theta})]$, in which the function $R(\boldsymbol{x}, \boldsymbol{x}_l, \boldsymbol{\theta})$ characterizes the correlation between $y(\boldsymbol{x})$ and $y(\boldsymbol{x}_l)$, with parameters $\boldsymbol{\theta}$ determined through maximum likelihood estimation based on $(\boldsymbol{X}, \boldsymbol{Y})$; $\boldsymbol{a}$ and $\boldsymbol{b}$ are constant coefficients obtained respectively through:

$$\begin{cases} \boldsymbol{a} = \left(\boldsymbol{F}^{\mathrm{T}}\boldsymbol{R}\boldsymbol{F}\right)^{-1}\boldsymbol{F}^{\mathrm{T}}\boldsymbol{R}^{-1}\boldsymbol{Y} \\ \boldsymbol{b} = \boldsymbol{R}^{-1}\left(\boldsymbol{Y} - \boldsymbol{F}\boldsymbol{a}\right) \end{cases} \tag{5}$$

where $\boldsymbol{F} = [\boldsymbol{f}(\boldsymbol{x}_1), \boldsymbol{f}(\boldsymbol{x}_2), ..., \boldsymbol{f}(\boldsymbol{x}_{n_\mathrm{s}})]^{\mathrm{T}}$; $\boldsymbol{R}$ is the correlation matrix with element (i, j) being $R(\boldsymbol{x}_i, \boldsymbol{x}_j, \boldsymbol{\theta})$.

In implementing this model, even though it is relatively time consuming to estimate $\boldsymbol{a}$, $\boldsymbol{b}$, and $\boldsymbol{\theta}$, owing to the matrix inversion or nonlinear optimization involved, this computational effort is unimportant in most applications, as $\boldsymbol{a}$, $\boldsymbol{b}$, and $\boldsymbol{\theta}$ only need to be calculated once for the training data set. Once the Kriging model is calibrated, the prediction, $\hat{y}(\boldsymbol{x})$, for a new input $\boldsymbol{x}$ can be estimated using Eq. (4) with negligible computational effort.

4. Real Time Damage Assessment

The calibrated Kriging metamodels, as presented in Section 3, are expected to provide reliable outputs at a much lower computational cost than the high-fidelity models, therefore enabling real time building envelope damage assessments during hurricane events. In particular, a circular region of radius r_r centered at the building site is first specified as the hurricane risk region. When there is an upcoming hurricane, the track of the hurricane center within the risk region is predicted in real time by the model reported in Vickery and Twisdale (1995). The wind field at each moment of interest is simulated based on the model proposed by Jakobsen and Madsen (2004). The wind speed $\bar{v}_H$ and direction α at the building site can then be obtained based on the simulated wind fields, as well as the relative location from the building site to the hurricane center. The building envelope damage, in terms of m_{G_C} and σ_{G_C}, can then be determined from the Kriging metamodels for the maximum wind speed and associated wind direction occurring over the whole predicted hurricane track.

5. Case Study

In this section, a case study is presented to illustrate the efficiency and accuracy of the Kriging metamodeling scheme, as well as its applicability to real time damage assessment.

5.1. *Building system and damage states*

The case study consists of a rectangular 45 story steel building assumed located in Miami, Florida, as outlined in Ouyang and Spence (2019) and illustrated in Figure 1. The story height for each floor is 4 m, leading to a total height of 180 m. Sections from the W24 American Institute for

Steel Construction (AISC) family and box sections are respectively considered for the structural beams and columns. The building was designed to satisfy an inter-story drift ratio limit of 1/400 under a 50-year mean recurrence interval (MRI) wind speed. The structural mass is evaluated based on an area density of 38 kg/m^2 distributed over the plane of each floor. The first three circular natural frequencies of the building were respectively 1.30 rad/s, 1.67 rad/s, and 2.70 rad/s.

The envelope system of the building is composed of 8,100 dual-pane laminated glazing elements (180 elements per floor). The size of all outer and inner laminated panes is 1.2×2 m^2 while the thickness is 6 mm. All elements are considered to be susceptible to inter-story drift ratios and net pressures. In particular, each envelope component is considered susceptible to two drift induced damage states, DS_1^{Dr} and DS_2^{Dr}, and one net pressure induced damage state, DS^p. The corresponding fragility functions were obtained from the FEMA P-58 guidelines (FEMA, 2012) and Behr et al. (1991), as summarized in Table 1. In particular, DS_1^{Dr}, DS_2^{Dr}, and DS^p correspond to the occurrence of hairline cracking, cracking, and blowout of the glazing panels. To further take into account the coupled nature of the damage, reduction factors, ρ, with means of 0.9 (10% reduction) and 0.2 (80% reduction) are considered for C^p upon the occurrence of DS_1^{Dr} and DS_2^{Dr}. In addition, ρ is assumed to follow a truncated normal distribution between $[0,\ 1]$, with a coefficient of variation of 0.1.

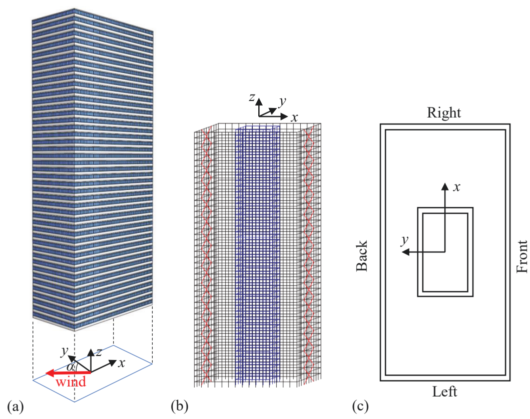

Fig. 1. Schematic of the building system: (a) the building envelope, (b) the structural system, and (c) plan view of the building.

Table 1. Fragility functions for the damage states.

DS	Statistics of the capacities C
DS_1^{Dr}	Median: 0.021; Dispersion: 0.45
DS_2^{Dr}	Median: 0.024; Dispersion: 0.45
DS^p	Mean: 5.29; Standard deviation: 0.91

Source: Units of DS_1^{Dr}, DS_2^{Dr}, and DS^p are respectively rad, rad, and kPa.

5.2. *Metamodel training and testing*

A set of support points was generated to define the training set for the Kriging metamodel. In particular, wind speed, $\bar{v}_H$, was considered to be within the range: $[43.90,\ 75.66]$ m/s, with upper and lower bounds corresponding to annual exceedance rates of 0.02 and 10^{-7} respectively. Within this context, a rectangular grid sampling plan in the space of $(\bar{v}_H, \alpha)$ was adopted, with 6 evenly sampled wind speed samples ranging from 43.90 m/s to 75.66 m/s and 36 wind directions corresponding to $\alpha = \{0°, 10°, 20°, ..., 350°\}$, leading to a total of 216 support points. At each support point, m_{G_C} and σ_{G_C} for each damage measure of each envelope element were estimated based on the procedure outlined in Section 2, while considering a sample size of 1000. These points defined the training data set. For the Kriging metamodel, the correlation function is taken as:

$$R(\boldsymbol{x}, \boldsymbol{x}_l, \boldsymbol{\theta}) = \exp\left(-\boldsymbol{\theta}^{\mathrm{T}}|\boldsymbol{x} - \boldsymbol{x}_l|^p\right) \tag{6}$$

where p is taken as 2 and implemented elementwise. In addition, a single constant term of 1 was considered for the basis function $\boldsymbol{f}(\boldsymbol{x})$ to capture the output means (Forrester et al., 2008). Kriging metamodels were constructed for $n_e = 300$ envelope elements of interest, as indicated in Figure 2.

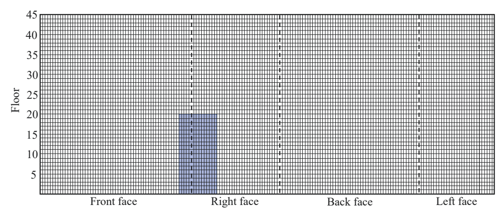

Fig. 2. Envelope elements of interest (shaded area).

To evaluate the performance of the metamodels, $n_{\mathrm{s}}^{\mathrm{te}} = 20$ samples of $(\bar{v}_H, \alpha)$ outside of the support points were generated as a test data set. In particular, a sample size of 1000 was again generated for each $(\bar{v}_H, \alpha)$ sample to evaluate m_{G_C} and σ_{G_C} while considering different random seeds from those used in obtaining the training

data set. All of the analyses were per
a personal computer with Intel(R) Co
8700 CPU @ 3.20 GHz processor a
RAM. Compared to the 28313 sec (3.
took to obtain the test data using the hi
model, the metamodels accurately rec
all results in only 0.66 s, demonstra
markable improvement in efficiency of
five orders of magnitude. Moreover, th
accurately provide all results with barel
putational effort using only a persona
illustrated the potential of the metamod
time damage assessment.

The accuracy of the metamodels wa
by the mean relative error, $\bar{E}_\mathrm{r}$, defined a

$$\bar{E}_\mathrm{r} = \frac{1}{n_\mathrm{e}} \sum_{k=1}^{n_\mathrm{e}} \left[\frac{\sum_{l=1}^{n_\mathrm{s}^\mathrm{te}} |y_k(\boldsymbol{x}_l) - \hat{y}_k(\boldsymbol{x}_l)|}{\sum_{l=1}^{n_\mathrm{s}^\mathrm{te}} |y_k(\boldsymbol{x}_l)|} \right] \quad (7)$$

where the subscript k indicates the kth envelope element of interest, $k = 1, 2, ..., n_\mathrm{e}$. The values of $\bar{E}_\mathrm{r}$ for the means, m_{G_C}, and standard deviations, σ_{G_C}, of $G_{C_1^{Dr}}$, $G_{C_2^{Dr}}$ and G_{C^p} are summarized in Table 2. It can be seen from Table 2 that the metamodels reproduced all the outputs with excellent accuracy over the test data set. In addition, the Kriging surface, training, and test data for the outputs of a representative envelope element are comparatively shown in Figure 3. As can be seen, the test data points are located perfectly on the Kriging surfaces. Furthermore, it can be noted that for all $G_{C_1^{Dr}}$, $G_{C_2^{Dr}}$ and G_{C^p}, the standard deviations had negligible variations over the input space of $(\bar{v}_H,\ \alpha)$. Therefore, for similar applications, a uniform standard deviation over the input space can be assumed without significantly compromising the accuracy.

Table 2. Mean relative error, $\bar{E}_\mathrm{r}$, for means and standard deviations of $G_{C_1^{Dr}}$, $G_{C_2^{Dr}}$ and G_{C^p}.

Outputs	$m_{G_{C_1^{Dr}}}$	$m_{G_{C_2^{Dr}}}$	$m_{G_{C^p}}$
$\bar{E}_\mathrm{r}$ (%)	2.12	2.05	0.95
Outputs	$\sigma_{G_{C_1^{Dr}}}$	$\sigma_{G_{C_2^{Dr}}}$	$\sigma_{G_{C^p}}$
$\bar{E}_\mathrm{r}$ (%)	4.10	4.10	2.68

5.3. *Real time damage assessment*

The applicability of the metamodels in real time damage assessment is demonstrated on the example building by considering an upcoming hurricane. In particular, the radius r_r of the hurricane

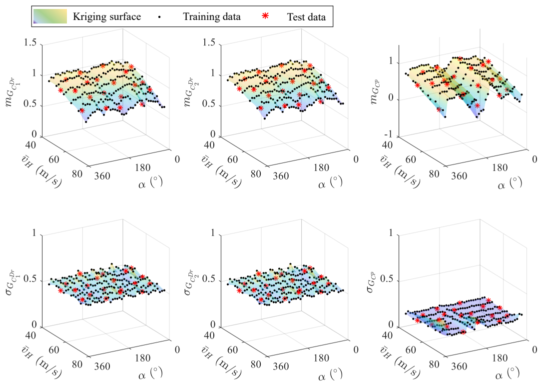

Fig. 3. Kriging surface, training, and test data for outputs of a representative envelope element.

risk region is taken as 250 km, as marked by the yellow circle in Figure 4(a). Based on Section 4, a hurricane track sample, as shown by the gray dashed line in Figure 4(a), as well as the evolution of the wind field, were generated within the risk region. The time histories of the wind speed, $\bar{v}_H$, and direction, α, at the site the building site were subsequently obtained based on the track sample and the corresponding wind field, as shown in Figure 4(b) and (c). The maximum wind speed and the corresponding direction were respectively 67.75 m/s and 54.63 °.

The building damage metrics, in the form of $m_{G_{C_1^{Dr}}}$, $\sigma_{G_{C_1^{Dr}}}$, $m_{G_{C_2^{Dr}}}$, $\sigma_{G_{C_2^{Dr}}}$, $m_{G_{C^p}}$, and $\sigma_{G_{C^p}}$, were obtained by the Kriging metamodels for the inputs of $\boldsymbol{x} = [67.75\ \mathrm{m/s}, 54.63\ °]^\mathrm{T}$, and are shown in Figure 5. It is seen that the Kriging metamodels are capable of providing comprehensive damage information for all the envelope elements of interest. In addition, it only took 0.37 s to evaluate the metamodels. The capability of accurately reproducing detailed damage information in real time has strong potential for real time damage assessment applications, which is of significant value for emergency response and management.

6. Conclusion

In this paper, a metamodeling scheme is presented for real time damage assessments of building envelope systems subject to hurricanes. In particular, the envelope damages are characterized by a recently proposed progressive multi-demand coupled fragility model, with multiple series of coupled damage states. For each damage state, a damage measure is defined while considering a full range of uncertainties in, e.g., structural properties, capacities, and wind load stochasticity. To overcome the computational difficulty associated with direct evaluation of the damage measures

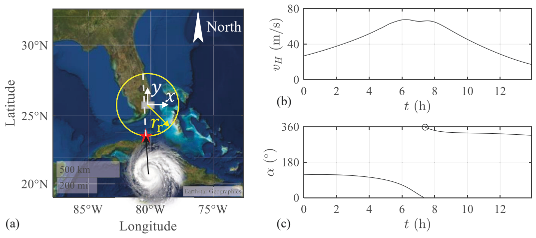

Fig. 4. The hurricane event: (a) predicted hurricane track (gray dashed line) within the hurricane risk region (the yellow circle) centered at the building (gray block); (b) predicted wind speed $\bar{v}_H$, and (c) direction α at the building location.

using high-fidelity models, Kriging metamodels are used to define the mapping from the input space of wind speed and direction to the output space of the means and standard deviations of damage measures for each envelope element. The significant gain in efficiency enables the real time prediction of building envelope damage information (in the form of means and standard deviations of damage measures) during hurricane events.

The efficiency and applicability of the developed scheme is illustrated on a case study consisting in a 45 story steel building. The calibrated metamodels are shown to be not only remarkably accurate but also more than five orders of magnitude faster than high-fidelity models. To further demonstrate the application to real time assessment, the building is assumed to be subject to an upcoming hurricane event. The calibrated metamodels are capable of providing comprehensive damage information on the building envelope nearly instantaneously, illustrating the strong potential of the proposed metamodeling scheme for real time damage assessments.

Acknowledgement

The research effort was supported in part by the National Science Foundation (NSF) under Grant No. CMMI-1562388 and CMMI-1750339 as well as the University of Michigan's Mcubed 3.0 program. This support is gratefully acknowledged.

References

Abdelhady, A. U., S. M. Spence, and J. McCormick (2020). A framework for the probabilistic quantification of the resilience of communities to hurricane winds. *Journal of Wind Engineering and Industrial Aerodynamics 206*, 104376.

Beason, W. L. and J. R. Morgan (1984). Glass failure prediction model. *Journal of Structural Engineering 110*(2), 197–212.

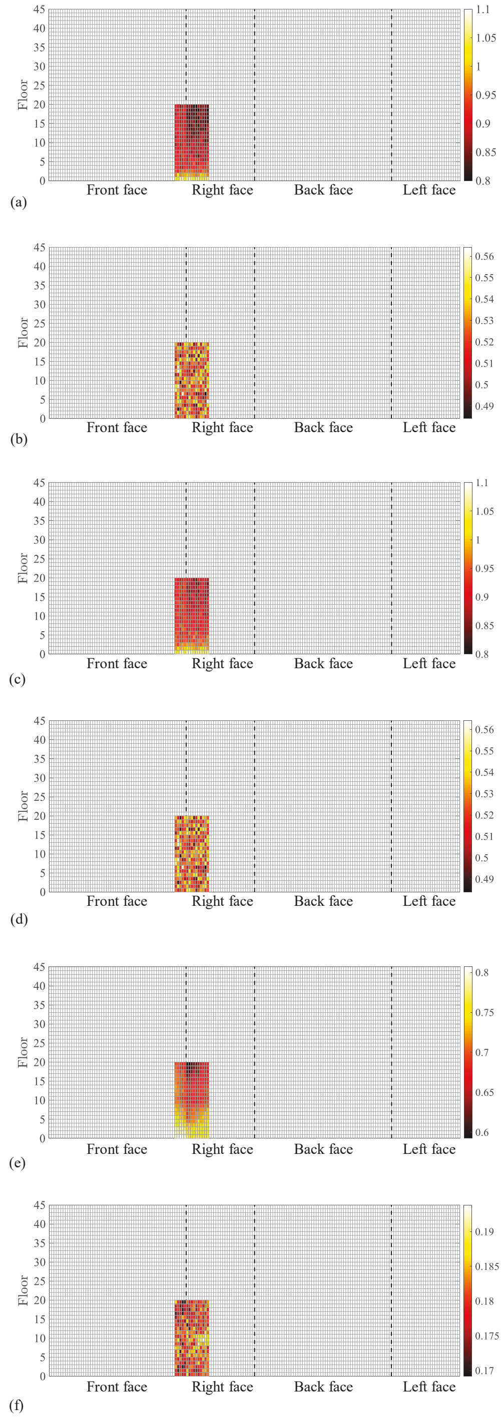

Fig. 5. Real time damage assessment results for each envelope element of interest: (a) $m_{G_{C_1^{Dr}}}$, (b) $\sigma_{G_{C_1^{Dr}}}$, (c) $m_{G_{C_2^{Dr}}}$, (d) $\sigma_{G_{C_2^{Dr}}}$, (e) $m_{G_{C^P}}$, and (f) $\sigma_{G_{C^P}}$.

Behr, R., M. Karson, and J. Minor (1991). Reliability analysis of window glass failure pressure data. *Structural safety 11*(1), 43–58.

Bevere, L. and M. Gloor (2020). *sigma 2/2020: Natural catastrophes in times of economic accumulation and climate change*. Swiss Re.

Box, G. E. and K. B. Wilson (1951). On the experimental attainment of optimum conditions. *Journal of the royal statistical society: Series b (Methodological) 13*(1), 1–38.

Emanuel, K. (2005). Increasing destructiveness of tropical cyclones over the past 30 years. *Nature 436*(7051), 686–688.

FEMA (2012). *Seismic performance assessment of buildings (volume 1-Methodology, FEMA P58-1)*, Volume 1.

Forrester, A., A. Sobester, and A. Keane (2008). *Engineering design via surrogate modelling: a practical guide*. John Wiley & Sons.

Ghosh, J., J. E. Padgett, and L. Dueñas-Osorio (2013). Surrogate modeling and failure surface visualization for efficient seismic vulnerability assessment of highway bridges. *Probabilistic Engineering Mechanics 34*, 189–199.

Guha, T., R. Sharma, and P. Richards (2011). Internal pressure dynamics of a leaky building with a dominant opening. *Journal of Wind Engineering and Industrial Aerodynamics 99*(11), 1151–1161.

Jakobsen, F. and H. Madsen (2004). Comparison and further development of parametric tropical cyclone models for storm surge modelling. *Journal of Wind Engineering and Industrial Aerodynamics 92*(5), 375–391.

Kameshwar, S. and J. E. Padgett (2014). Multi-hazard risk assessment of highway bridges subjected to earthquake and hurricane hazards. *Engineering Structures 78*, 154–166.

NOAA (2013). *National Coastal Population Report: Population Trends from 1970 to 2020*. National Oceanic and Atmospheric Administration.

Ouyang, Z. and S. M. Spence (2019). A performance-based damage estimation framework for the building envelope of wind-excited engineered structures. *Journal of Wind Engineering and Industrial Aerodynamics 186*, 139–154.

Ouyang, Z. and S. M. Spence (2020). A performance-based wind engineering framework for envelope systems of engineered buildings subject to directional wind and rain hazards. *Journal of Structural Engineering 146*(5), 04020049.

Ouyang, Z. and S. M. Spence (2021). Performance-based wind-induced structural and envelope damage assessment of engineered buildings through nonlinear dynamic analysis. *Journal of Wind Engineering and Industrial Aerodynamics 208*, 104452.

Powell, M. D., S. H. Houston, L. R. Amat, and N. Morisseau-Leroy (1998). The hrd real-time hurricane wind analysis system. *Journal of Wind Engineering and Industrial Aerodynamics 77*, 53–64.

Sacks, J., W. J. Welch, T. J. Mitchell, and H. P. Wynn (1989). Design and analysis of computer experiments. *Statistical science*, 409–423.

Saha, S. K., V. Matsagar, and S. Chakraborty (2016). Uncertainty quantification and seismic fragility of base-isolated liquid storage tanks using response surface models. *Probabilistic Engineering Mechanics 43*, 20–35.

Seo, J., L. Dueñas-Osorio, J. I. Craig, and B. J. Goodno (2012). Metamodel-based regional vulnerability estimate of irregular steel moment-frame structures subjected to earthquake events. *Engineering Structures 45*, 585–597.

Taflanidis, A. A., A. B. Kennedy, J. J. Westerink, J. Smith, K. F. Cheung, M. Hope, and S. Tanaka (2013). Rapid assessment of wave and surge risk during landfalling hurricanes: Probabilistic approach. *Journal of waterway, port, coastal, and ocean engineering 139*(3), 171–182.

Towashiraporn, P. (2004). *Building seismic fragilities using response surface metamodels*. Ph. D. thesis, Georgia Institute of Technology.

Vickery, B. and C. Bloxham (1992). Internal pressure dynamics with a dominant opening. *Journal of Wind Engineering and Industrial Aerodynamics 41*(1-3), 193–204.

Vickery, P. J. and L. A. Twisdale (1995). Prediction of hurricane wind speeds in the united states. *Journal of Structural Engineering 121*(11), 1691–1699.